International Journal of Heat and Mass Transfer 51 (2008) 5975–5982

Contents lists available at ScienceDirect

International Journal of Heat and Mass Transfer

journal homepage: www.elsevier.com/locate/ijhmt

Frost formation on a super-hydrophobic surface under natural convection conditions

Zhongliang Liu *, Yunjun Gou, Jieteng Wang, Shuiyuan Cheng

Key Laboratory of Enhanced Heat Transfer and Energy Conservation, Ministry of Education (also Key Laboratory of Heat Transfer and Energy Conversion, Beijing Education Commission), College of Environmental and Energy Engineering, Beijing University of Technology, Beijing 100022, PR China

ARTICLE INFO

Article history:
Received 6 November 2007
Received in revised form 28 March 2008
Available online 2 June 2008

Keywords:
Super-hydrophobic surface
Lotus effect
Frost deposition
Contact angle

ABSTRACT

In this paper, the frost deposition phenomena on a cold super-hydrophobic surface whose contact angle with water is 162° were observed of the formation of water droplets, the freezing process, the formation of initial frost crystals and the frost layer structure. The frost layer structure formed on the super-hydrophobic surface shows remarkable differences to that on a plain copper surface: the structure is weaker, looser, thin and easy to be removed and most importantly, it is of a very special pattern, a pattern similar to a cluster of chrysanthemum petals, a frost layer structure that has not been reported before. The experimental results also show that the surface has a strong ability to restrain frost growth. The frost deposition on the surface was delayed for 55 min compared with the plain copper surface under the tested conditions.

1. Introduction

Frost formation phenomenon is often encountered when a cold surface with a temperature below air dew point is exposed to humid air. Frosting will also ensue if the surface temperature is below freezing point. This phenomenon is undesirable due to the insulation effects of the frost layer along with the reduction in heat transfer and airflow area that results in an increase in pressure loss. Therefore, many researchers have tried to find effective methods to prevent frost formation. Among these methods, innovative surface technology that will prevent frost particles from sticking to the surface is a highly desired means of alleviating the frost deposition problem. Forest [1] evaluated the use of polymer coatings to reduce the surface energy, which resulted in a reduced ice adherence force. He concluded a "zero surface energy" coating should meet this goal. If the surface energy is zero, the contact angle (CA) should be 180°. Teflon is usually considered as a low surface energy coating, but its contact angle is not large enough to prevent frost adherence.

Recently, with the rapid development of advanced material science and technology, a bionic super-hydrophobic surface technology was developed. By use of this surface technology a surface with extra-large contact angle can be manufactured. The resulted surface is of a highly multiple micro–nano-binary structure similar to the microstructure of a natural lotus leaf surface. The contact angle of water on this surface is greater than 150° and its roll angle is smaller than 5°. The research on this kind of surfaces was first illumined by the self-cleaning characteristics of natural lotus leaves. This phenomenon was first put forward by Barthlott [2], a botanist in the University of Bonn and Barthlott named this phenomenon as lotus effect. Since then, many studies were carried out and focused on the manufacture and the self-cleaning effect of the surfaces. Recently, super-hydrophobic surfaces were fabricated successfully with nano-structured polymers [3–5]. Scientists have successfully made this kind of bionic coating on various metal surfaces [6,7]. As we know, frost deposition on cold solid surface is a typical interface phenomenon and thus the surface characteristics should have strong influences on the frost deposition process. Actually, many research work have already disclosed that the contact angle of water on the solid surface has a direct effect on the frost deposition process and the large contact angle surface may significantly retard or restrain the initial frost crystal nucleation [8]. This paper reports the experimental results of the frost deposition phenomena of the super-hydrophobic surface.

2. Experimentation

2.1. Experimental apparatus

Fig. 1 illustrates the experimental apparatus. The experimental setup mainly consists of cooling setting, microscopic image system,

* Corresponding author. Address: Key Laboratory of Enhanced Heat Transfer and Energy Conservation, Ministry of Education, College of Environmental and Energy Engineering, Beijing University of Technology, Beijing 100022, PR China. Tel.: +86 10 67391917; fax: +86 10 67391983.
E-mail address: liuzl@bjut.edu.cn (Z. Liu).

0017-9310/$ - see front matter © 2008 Elsevier Ltd. All rights reserved.
doi:10.1016/j.ijheatmasstransfer.2008.03.026

data acquisition system, a digital camera, optical fiber luminescence, air condition and humidity controller.

The cooling system is basically a thermoelectric cooler. It can provide cooling to maintain the cold plate temperature from 0 °C to −26 °C. A test sample plate that has a super-hydrophobic surface on the left half part and the plain copper surface on the right half was embedded on the cooled plate. The surfaces were all placed horizontally with the cold surface on the topside. The surface temperature of the cold plate was measured by 4 T-type thermocouples that were buried beneath the test surface through 4 holes of 1 mm in diameter and 13 mm in depth drilled into the plate. The temperature data recorded by a HP data acquisition system was finally transferred to a personal computer for further analysis. The cold surface temperature was the average of the temperature readings of the four thermocouples. The thermocouples were calibrated in advance and the estimated uncertainty of the cold plate surface temperature is less than 0.5 °C, including those resulted from the location errors. The contact angle was measured by a FTA32 contact angle measuring system that uses a side profile image to determine the contact angle with an uncertainty of 0.1°.

The test surfaces and the thermoelectric cooler were placed in a large Plexiglas enclosure to maintain pure natural convection condition during the test. The temperature and the humidity inside the enclosure were regulated at the given value by an air-condition system and a humidity controller. A thermo-hygrometer was used to measure the relative humidity with an uncertainty of 1%.

The microscopic image system consists of a CCD camera, a microscope and a capture card. The system was used for the micro and transient observations of the frost deposition process and for the measure of the frost layer thickness. The CCD camera and microscope with a maximum magnification of 110 were mounted right over the cooled surface to take photographs and observe the frost formation with the help of an optical fiber luminescence. The frost deposition process was recorded by the microscopic image system at a speed of 30f/s. And the frost layer thickness is measured by a micro-measurement system that is integrated into the microscopic image system every 5 min and is of an accuracy of ±0.05 mm.

2.2. Experimental procedure

The super-hydrophobic surface was supplied by the College of Material Science and Technology, Beijing University of Technology. Hydrophobic a-C films with lotus-leaf-like surface structure were fabricated on Si(1 0 0) substrates by a magnetron sputtering system. The super-hydrophobic surface was then obtained by a rapid fluorinated process of carbon tetrafluoride (CF_4) plasma. The surface morphology of the surface is observed by an atomic force microscope (Molecular Image # Pico Scan Z500) and the results are shown in Fig. 2a (two-dimensional structure) and Fig. 2b (three-dimensional structure). Fig. 2c illustrates a water droplet on the surface, which shows that the surface has a very large contact angle (the measured contact angle is 162°) and thus is of super-hydrophobicity.

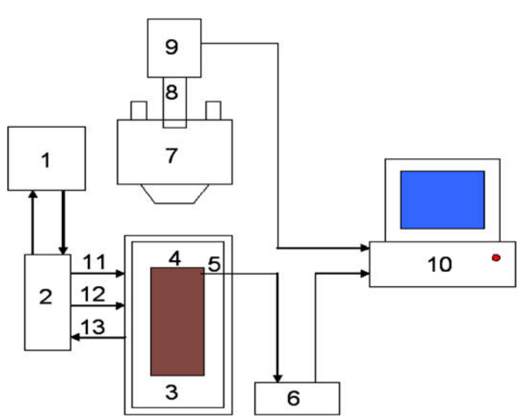

Fig. 1. Experimental system and apparatus: (1) cooling water source; (2) power source for thermoelectric cooler; (3) cold plate; (4) thermoelectric cooler; (5) T-type thermocouples; (6) HP data acquisition system; (7) microscope; (8) camera lens; (9) CCD; (10) computer; (11) power supply cable; (12) water inlet; (13) water outlet.

The sample plate with the super-hydrophobic surface used in this research has a contact angle of 162°, and the plain copper surface has a contact angle of 72°, the sample plate was embedded on the cooled plate of the thermoelectric cooler.

The temperature and frost formation were recorded every 60 s. The air inside the enclosure was maintained at 18.4 °C, and the air relative humidity at 40%. The cold plate temperature was −10.1 °C. Before the cooling process of the cold plate from the room temperature to the given temperature was initiated, a soft and thin plastic film was used to cover the sample surfaces to prevent vapor in air from condensing on the surfaces. After the given temperature of the cold plate was acquired, the plastic film was taken away from the surface to start a test. During the test, the frost deposition process on both the super-hydrophobic and the plain copper surface was observed and recorded. The structure of the frost layer or crystals on both the parts of the surface was obtained by a digital camera via the microscope. The test lasted for 2 h.

3. Experimental results and discussion

3.1. Results

From the experimental observation and measurements, we found that the time for the first observable condensate droplet, the diameter of the condensate droplet, the start time for the condensate droplet freezing, the time for the first observable frost crystal, the shape of the frost crystals and the structure pattern of the frost layer formed at the end of the test were completely different from each other on the super-hydrophobic and the plain copper surface. Fig. 3 shows some of the typical pictures of the condensate droplets and frost formation on the two surfaces during the test. The left half of each picture is the super-hydrophobic surface and the right half is the plain copper surface. The main results are summarized as follows.

The first observable condensation water droplet from air on the super-hydrophobic surface appears much later than that on the plain copper surface. On the plain copper surface, the first observable condensate droplet appears at 30 s after the test starts and then, at about 60 s these droplets freeze into ice. However, on the super-hydrophobic surface the first observable condensate droplet appears much later, actually, it is only at about 620 s that a small number of condensate droplets begin to appear. The size of the droplets formed on the left half (the super-hydrophobic part) grows steadily remaining their liquid state, they keeps unfrozen as long as 30 min. However, during the same period of time, the whole plain copper surface (the right half) has been already covered by a continuous frost layer as shown in Fig. 3.

The time needed for the formation of a continuous frost layer on the super-hydrophobic surface is therefore much longer than that on the plain copper surface. As have been already mentioned, the liquid droplets formed on the plain copper surface were frozen at only about 1 min after the starts. However, it is until 55 min that the condensate droplets of large sizes on the left super-hydrophobic surface begin to freeze, though at this time the left part of the surface is completely covered by a thick and dense frost layer. Fig. 4a and b compares the frost layer structures on the super-

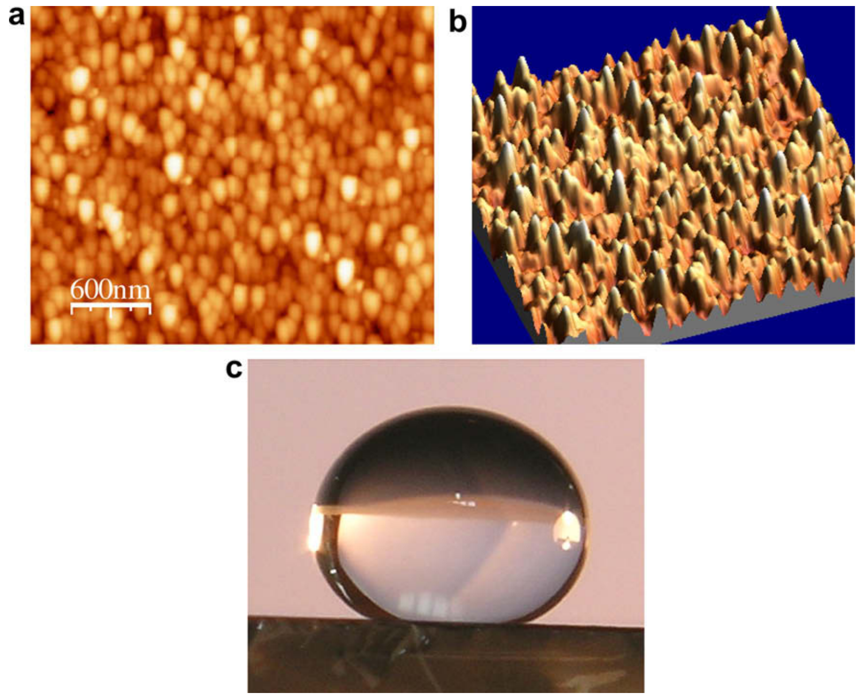

Fig. 2. Morphology of the test surface: (a) two-dimensional AFM imaging of the surface; (b) three-dimensional AFM imaging of the surface; (c) a water droplet on the surface.

hydrophobic (the left half) and the plain copper surface (the right half) at 70 min and 120 min, respectively.

After the water droplets on the left half surface are frozen, it is observed that frost crystals begin to grow on these frozen water droplets just like on the plain copper surface. But the way that the frost crystals grow on the super-hydrophobic surface is different to that on the plain copper surface. The frost crystals grow along different directions. On the super-hydrophobic part of the left half, most of the frost crystals grow along the horizontal direction (parallel to the surface) instead of the normal vertical direction (normal to the surface) as those on the plain copper surface of the right half. The frost crystals arranged in a chrysanthemum-like pattern. Fig. 4c and d presents the pictures of the more detailed structure of this peculiar frost crystal pattern on the super-hydrophobic surface. As one can see from these pictures, on the super-hydrophobic surface, frost crystals show much of directional growth than on the plain copper surface. Actually, as far as the authors could know, the observed peculiar pattern of the frost layer structure has not been reported before.

The frost layer growth was also recorded during the experiment. Fig. 5 compares the frost layer thickness on the super-hydrophobic surface with that on the plain copper surface. From this figure, we can see that the super-hydrophobic surface delays the frost crystal formation for 55 min and therefore this surface as one may expect has a very strong ability to restrain frost formation. Actually, our experimental measurement shows that the frost thickness reduction of the super-hydrophobic surface compared with the plain copper surface is 52% at the end of the test.

In order to find why the frost crystals grow along the horizontal direction (parallel to the surface) on the super-hydrophobic surface, we designed the following test. We put a droplet on the super-hydrophobic surface and the copper surface each with an injector needle tube and observed the droplet freezing process and frost crystal growth on the droplet surface. The diameters of these two droplets are 1 mm and 1.5 mm, respectively. The air inside the enclosure was maintained at 17.5 °C, and the relative humidity at 42%. The cold plate temperature was −10.4 °C. During the test, freezing of the droplets on the two different surfaces and the frost crystal growth on the two frozen droplets surface were observed. The test lasted for 90 min. The droplet shapes on the two surfaces are very different as shown in Fig. 6a and b. At about 450 s and 440 s after the test started the two droplets both freeze into ice and small protrusions appear on the top of the two droplets at the end of the freezing process as shown in Fig. 6c and d. It is postulated that the effects of surface tension and volume dilatation resulted from liquid-to-solid phase change caused the shape change and protrusions formation [9]. Then at about 970 s and 985 s frost crystals appear on the protrusion of the droplets on the two surfaces as shown in Fig. 6g and h. During this period, droplet freezing into ice and appearance of frost crystals on the two surfaces are very similar. But after the droplets are frozen, the phenomena happening on the two droplet surfaces are quite different. On the super-hydrophobic surface the frost crystals grow on almost every position of the ice droplet surface as shown in Fig. 6i and k. But on the copper surface the frost crystals grow mainly on the top of the ice droplet and along the vertical direction as shown in Fig. 6j and l. At about 3920 s, the frost crystals flourish on the whole surface of the droplet on the super-hydrophobic surface as shown in Fig. 7a. Then at about 5410 s the frost crystals on the upper position of the droplet thawed and fell down onto the crystals of the lower part of the droplet on the hydrophobic surface, as shown in the red ring in Fig. 7b. This phenomenon was not observed on the copper surface and would certainly enhance the growth of the frost crystals in the horizontal direction.

3.2. Discussions

The experimentally observed phenomena are closely related to the water wettability of various surfaces and the sub-micron scale structure of the super-hydrophobic surface. The surface wettability is measured by contact angle. If the contact angle of a surface with water is less than 90° and the surface is tending to wetting then the surface is usually classified as hydrophilic, otherwise, if a surface's contact angle with water is greater than 90° and the surface is

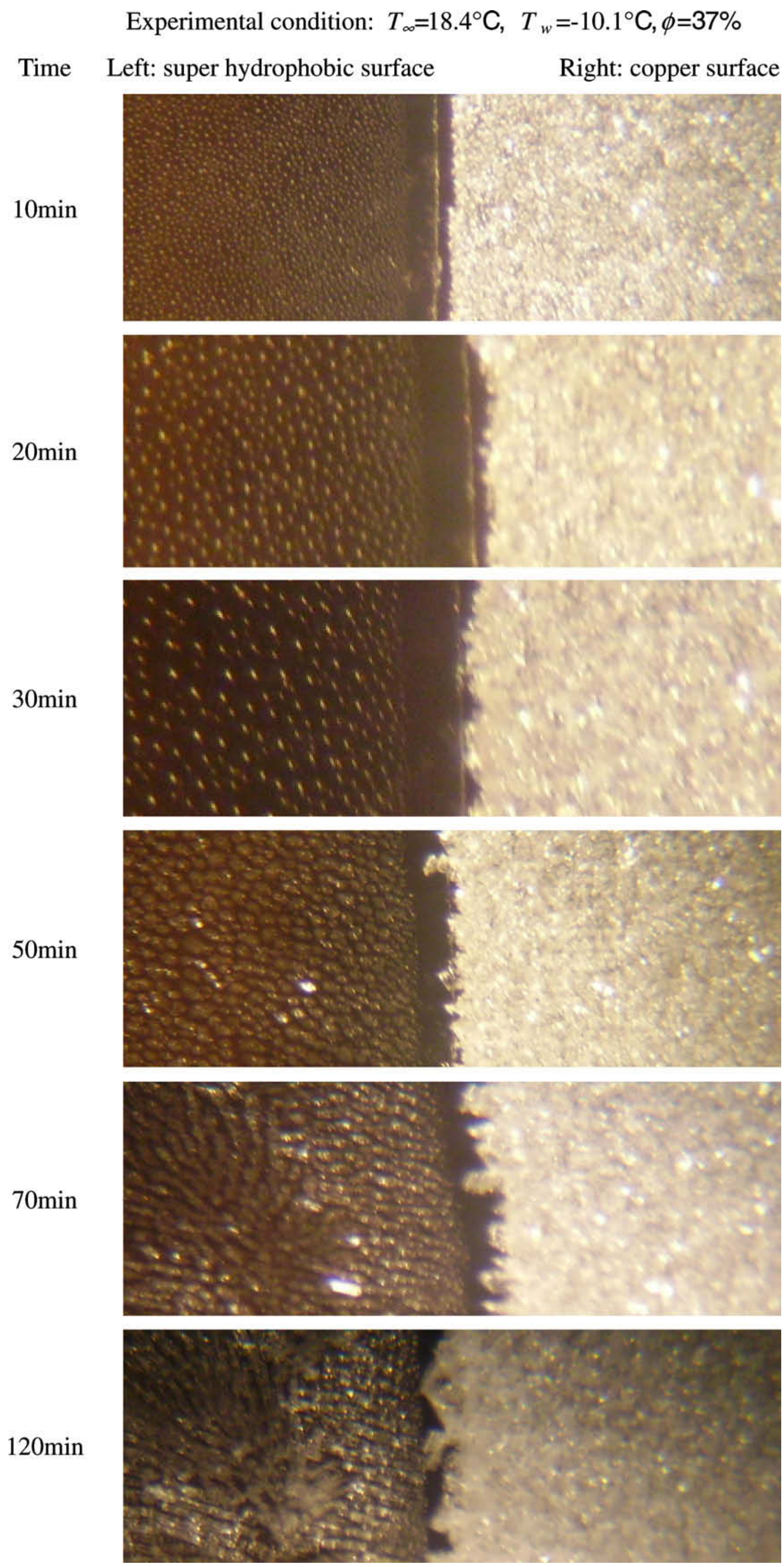

Fig. 3. The observed frost layer growth process on both the super-hydrophobic super-hydrophobic surface (the left half) and the plain copper surface (the right half).

tending to non-wetting, then it is usually classified as hydrophobic. And, if a surface whose contact angle is greater than 150°, then it is regarded as super-hydrophobic. Contact angle of water on a surface is determined mainly by the characteristics of the solid sur-

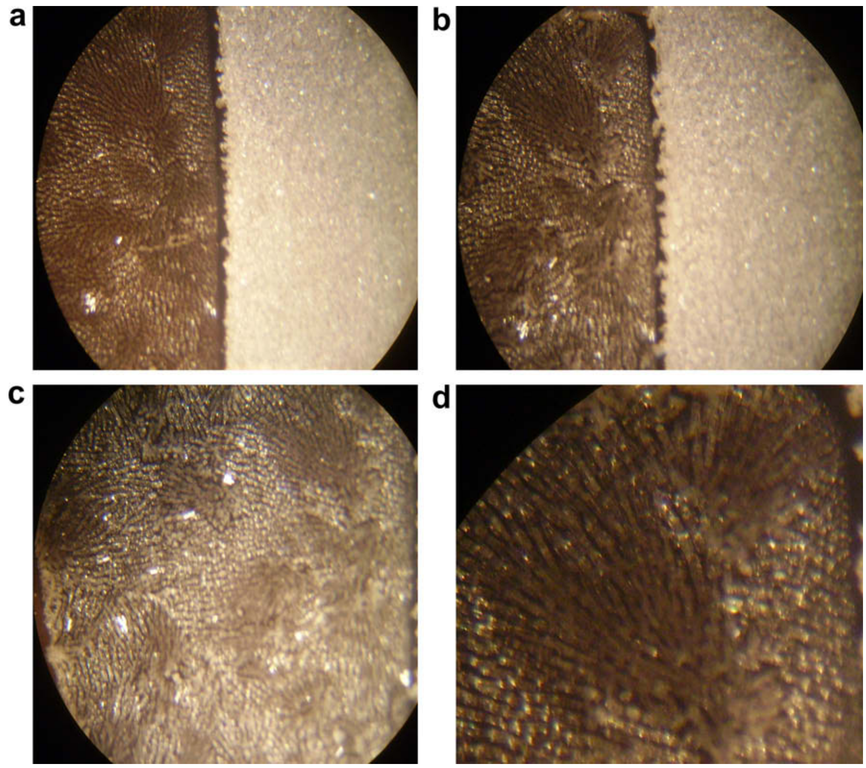

Fig. 4. Comparison of the frost layer structure of the super-hydrophobic surface (the left half) with that of the plain copper surface (the right half): (a) 70 min; (b) 120 min; (c) general view of the frost layer structure formed on the super-hydrophobic hydrophobic surface; (d) a cluster of frost crystals shows a chrysanthemum-petal-like pattern on the super-hydrophobic hydrophobic surface.

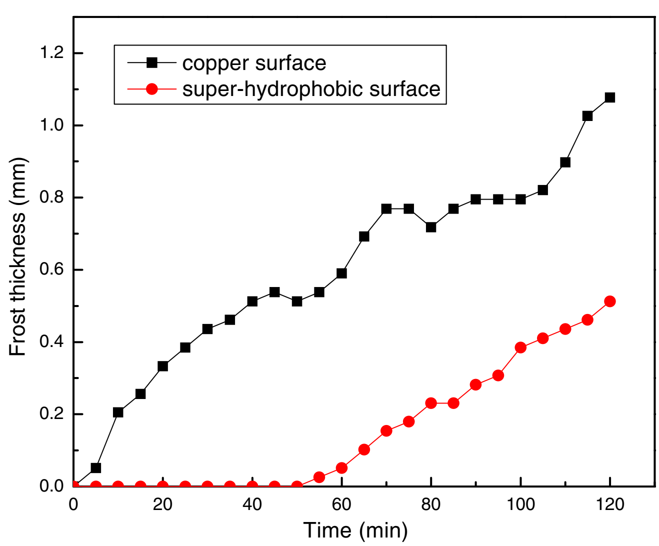

Fig. 5. Frost thickness versus time.

face. For an ideal surface, which is absolutely smooth, the relationship between contact angle θ and surface tension σ can be described by the famous Young equation [10]:

$$\cos\theta = \frac{\sigma_{sv} - \sigma_{sl}}{\sigma_{lv}} \quad (1)$$

where σ_{sv}, σ_{sl} and σ_{lv} are the surface tension between solid and vapor phase, the surface tension between solid and liquid phase and the surface tension between liquid and vapor phase, respectively. For real or non-ideal surfaces which are not absolutely smooth, Wenzel [11] modified Eq. (1) by introducing a correction factor with the consideration of the surface roughness and the following equation was proposed:

$$\cos\theta' = \gamma\frac{\sigma_{sv} - \sigma_{sl}}{\sigma_{lv}} \quad (2)$$

where γ is the Wenzel correction factor and is always greater than unity. It can be shown that the Wenzel correction factor is equal to the ratio of the real or actual contact area between a liquid drop and the solid surface to the apparent contact area on a perfect smooth surface under the same conditions. The Wenzel model explains fact that the contact angle θ' on a real hydrophobic surface is always greater than that on its corresponding perfect smooth surface. However, it fails to describe the phenomenon that the contact angle θ' on a real hydrophilic surface can also be greater than that on its corresponding perfect smooth surface.

Later, Cassie and Baxter [12] studied many kinds of hydrophobic surfaces in the nature and presented a gas cavity model for surface wettability as shown in Fig. 8. When a liquid droplet gets contacted with a solid surface, the micro-groves that inevitably exist on the surface could not fill with liquid due to the effects of liquid surface tension, instead, they are full of air. Therefore, the contact area between a liquid droplet and a solid surface consists of two parts, the contact area between the droplet and the small micro-bumps of the solid surface and the area between the droplet and the air in the micro-grooves of the solid surface. Based on these considerations, they developed the following equation for the real surface contact angles:

$$\cos\theta' = f\cos\theta + f - 1 \quad (3)$$

where θ' is the contact angle for real surfaces and θ is the contact angle for ideal surfaces, f is the ratio of the contact area of a droplet with micro-bumps to the total contact area. Since f is always smaller than unity, the contact angles of real surfaces are therefore always greater than that of ideal surfaces under the same

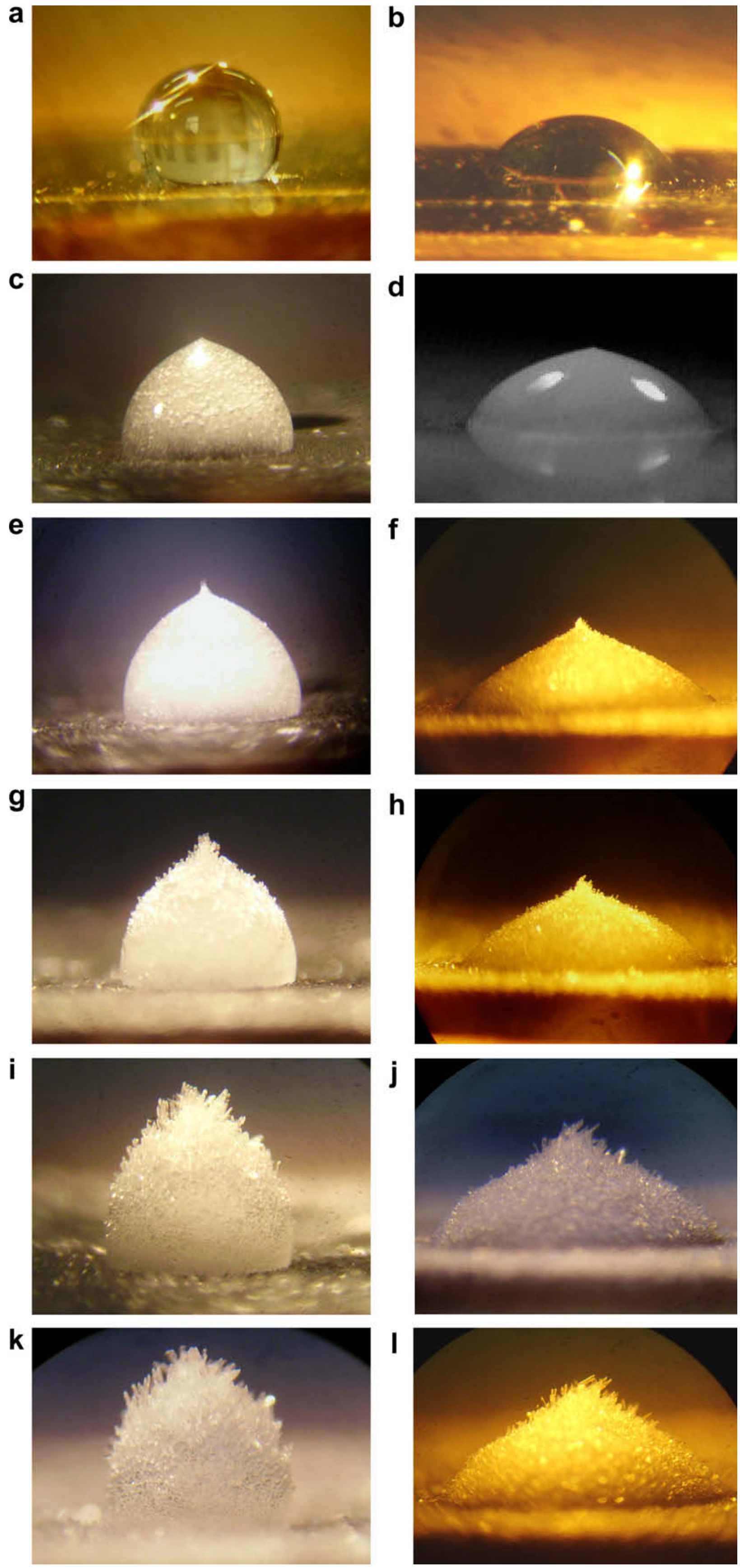

Fig. 6. Formation of frost crystals on two frozen water droplets surfaces on both the super-hydrophobic and the copper surface ($T_w = -10.4$ °C, $\phi = 42\%$, $T_\infty = 17.5$ °C). (a) Before cooling: water droplet on the super-hydrophobic surface; (b) before cooling: water droplet on the copper surface; (c) 450 s, super-hydrophobic surface; (d) 440 s, copper surface; (e) 555 s, super-hydrophobic surface; (f) 585 s, copper surface; (g) 970 s, super-hydrophobic surface; (h) 985 s, copper surface; (i) 2199 s, super-hydrophobic surface; (j) 2186 s, copper surface; (k) 3025 s, super-hydrophobic surface; (l) 3090 s, copper surface.

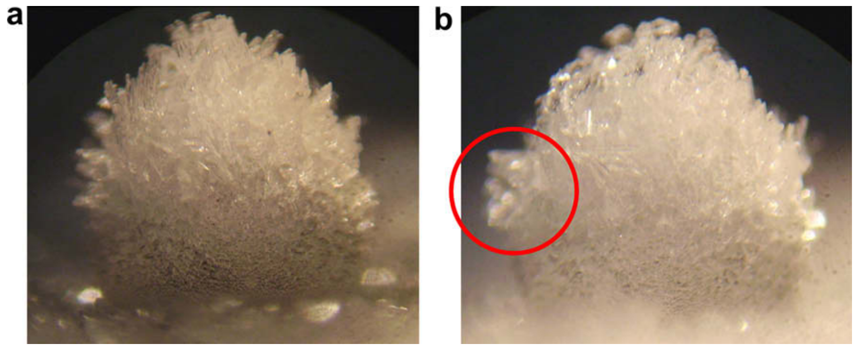

Fig. 7. Frost crystal growth on the super-hydrophobic surface of the later period: (a) frost crystals flourish at about 3920 s; (b) thawing and falling down of frost crystals at about 5410 s.

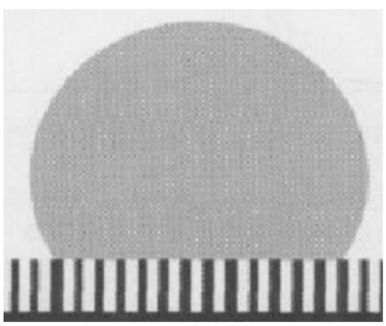

Fig. 8. Cassie model for surface wettability.

conditions. This equation also tells us by reducing the fractional contact area of a liquid droplet with micro-bumps or increasing the fractional area of the micro-grooves we actually can increase contact angles of a liquid.

The lotus leaves are super-hydrophobic due to the presence of multiple micro–nano-binary (100–200 nm) rough structures and a thin wax film on the surface of the leaves. Many micro-bumps were observed on lotus leaf surface and a good deal of fine villosities distributed on these bumps' surface. On the top of each bump there is a tip. The micro-grooves among these bumps were filled with air, and thus many extremely small gas cavities with nano-sized volume formed on the leaf surface. Liquid droplets can only contact with these micro-bumps on lotus leaves. Therefore, the value of f is very small, usually between 0.02 and 0.03. Hence, the contact angle is very large, in the extreme cases, it can be as big as 172°.

As we know, contact angle has a very direct and strong influence on various phase transition phenomena. It is usually considered that the frost deposition process actually starts from the condensation of vapor in the most situations, i.e., the vapor is first cooled down to condense on the cold surface to form water droplets of various sizes and then after a period of time the water droplets on the cold surface freezes and after that the frost deposition begins [13–16]. Therefore, the contact angle will certainly affect the frost formation process by influencing vapor condensation on the cold surface. As phase transition theory tells us, a water droplet and thus a frost crystal can appear, exist and grow up on a surface only if its size is larger than its critical radius [17]. Phase transition can happen only if the process results in a decrease in Gibbs free energy of the system. If the initial water droplet size is larger than its critical radius, the Gibbs free energy decreases as the water droplet grows. Supersaturated vapor in air is a metastable phase and the water droplet is a stable phase during the initial period of the frost formation process. For supersaturated vapor to change from its metastable phase into the stable phase (liquid water) a so-called potential barrier, i.e. the Gibbs free energy difference ΔG_c must be overcome. Only when the potential barrier is exceeded, can the new water droplet nucleus be formed and grow. If a shape of spherical cap is assumed for a water droplet formed on a flat cold surface, then the potential barrier that must be overcome is [17]:

$$\Delta G_c = \frac{4\pi}{3}\left[\frac{2\sigma_{vl}}{\rho_l R_w T \ln(p/p_{sl})}\right]^2 \sigma_{vl} f(\theta) \tag{4}$$

where

$$f(\theta) = \frac{1}{4}(2+\cos\theta)(1-\cos\theta)^2 \tag{5}$$

ρ_l is the density of liquid phase, kg/m^3; T is the surface temperature, K; p is the vapor pressure, Pa; p_{sl} is the saturated vapor pressure corresponding to the surface temperature T, Pa and R_w is gas constant for water, J/(kg K). From Eq. (4) we can see that the value of function $f(\theta)$ directly determines the potential barrier. From Eq. (5) one can see that $f(\theta)$ is a single-valued function of the contact angle θ. It can also be shown that $f(\theta)$ is a monotonously increasing function of contact angle. $f(\theta)$ acquires its maximum value at $\theta = 180°$. Hence, increasing the contact angle of a surface will increase the potential barrier, and thus restrain the frost crystal nucleation. For ordinary hydrophobic surfaces, the contact angle is usually smaller than 110°, and on such surfaces the potential barrier is about 8.8 times of the common metallic surfaces with a contact angle of 50°. Our super-hydrophobic surface used in the present test has a contact angle of 162°, its potential barrier is as large as 11.8 times of the common metallic surfaces. This explains why our super-hydrophobic surface has a very strong ability to restrain frost formation. It can delay the frost nucleation for as long as 55 min compared with the plain copper surface.

From the freezing process of the water droplets, we observed that the frost crystal growth on the frozen droplets that were dripped onto the super-hydrophobic surface and the copper surface shows a significant difference. The frost crystals grow on much larger portion of the frozen water droplet surface on the super-hydrophobic surface than on the plain copper surface. And the frost crystal growth on the super-hydrophobic surface presents of much more dendritic growth.

We also observed that thawing may happen as frost crystals grow. This might be caused by the perturbation of air flow. At the upper part of the droplet on the super-hydrophobic surface thawing phenomenon happens more easily than at the lower part of the droplet. This is not only because that the frost crystals at the lower part are of lower temperature, but also because they have little chance to get contacted with the air flow. So even the frost crystals on the upper part thawed and fell down onto the frost crystals on the lower part of the droplet, the frost crystals on the lower part may well remains unthawed. As a result, the frost crystals on the lower part grow faster and become stronger. This in turn enhances the horizontal growth of the frost crystals. If there are many such droplets on the super-hydrophobic surface as observed in our frost deposition experiment, the frost crystals on the lower part of droplets will connect with each other, and accelerate the formation of frost crystals on the lower part of the droplets. This perhaps explains why on the super-hydrophobic surface we observed the very peculiar frost layer structure.

4. Concluding remarks

The frost deposition on the super-hydrophobic surface was studied and a very special frost layer structure was observed. On the super-hydrophobic surface with a contact angle of 162°, the frost crystals grow along the horizontal direction (parallel to the surface) around a center and finally show a chrysanthemum-like pattern. The possible theory was proposed to explain the observed phenomena: it may be related to the facts that water molecules are of strong polarity and the electric charge distribution is non-uniform on an isolated conductor surface. The frost layer thickness was also measured and it was shown that the frost deposition was delayed for 55 min compared with the plain copper surface under the conditions of cold plate temperature −10.1 °C, air temperature 18.4 °C and relative humidity 40%.

Acknowledgements

This work is supported by the Chinese National Natural Science Foundation Project No. 50376001, Beijing Outstanding Scholar Program (2006), Beijing Natural Science Foundation Project No. 3073014, the Beijing Science and Technology Plan and Development Project and the Key Project No. 2005CB724201 of The National Fundamental Research and Development Program, The Ministry of Science and Technology of The People's Republic of China.

References

[1] T.W. Forest, The adhesion of ice to low energy solids, in: ASME Winter Annual Meeting on Heat Transfer, Chicago, November 1980, paper 80-WA/HT-19.
[2] W. Barthlott, C. Neinhuis, Purity of the sacred lotus or escape from contamination in biological surface, Planta 202 (1) (1997) 1–8.
[3] N.J. Shirtcliffe, G. Mchale, M.I. Newton, G. Chabrol, C.C. Perry, Dual-scale roughness produces unusually water repellent surfaces, Adv. Mater. 16 (2004) 1929.
[4] L. Feng, Y.L. Song, J. Zhai, B.Q. Liu, J. Xu, L. Jiang, D.B. Zhu, Creation of a superhydrophobic surface from an amphiphilic polymer, Angew. Chem. Int. Edit. 42 (2003) 800–802.
[5] Q.D. Xie, G.Q. Fan, N. Zhao, X.L. Guo, J. Xu, J.Y. Dong, L.Y. Zhang, Y.J. Zhang, C.C. Han, Facile creation of a bionic super-hydrophobic block copolymer surface, Adv. Mater. 16 (2004) 1830.
[6] C.H. Su, Y. Xiao, Z. Cui, A simple way to fabricate multi-dimension bionic super-hydrophobic surface, Chin. J. Inorg. Chem. 22 (5) (2006) 785–788.
[7] M.Y. Song, X.T. Huang, Experimental research to fabricate super hydrophobic aluminum surface, J. Yangtze Univ. (Nat. Sci. Edit.) 3 (4) (2006) 28–30.
[8] X. Wang, S. Jiang, Discussions on hydrophobic surface for preventing frosting and speeding defrosting of heat pump, Energy Conserv. Technol. 22 (127) (2004) 37–38.
[9] J.T. Wang, Z.L. Liu, Y.J. Gou, Deformation of freezing water droplets on a cold copper surface, Sci. China (Ser. E) 49 (5) (2006) 590–600.
[10] T. Young, An essay on the cohesion of fluids, Philos. Trans. Royal Soc. London 95 (1805) 65–87.
[11] R.N. Wenzel, Resistance of solid surface to wetting by water, Ind. Eng. Chem. 28 (8) (1936) 988–994.
[12] A. Cassie, S. Baxter, Wettability of porous surfaces, Trans. Faraday Soc. 40 (1944) 546–551.
[13] B. Na, R.L. Webb, A fundamental understanding of factors affecting frost formation, Int. J. Heat Mass Transfer 46 (2003) 3797–3808.
[14] J. Shin, A.V. Tikhonov, C. Kim, Experimental study on frost structure on surfaces with different hydrophilicity: density and thermal conductivity, J. Heat Transfer, ASME Trans. 125 (2003) 84–94.
[15] J.L. Hoke, The interaction between the substrate and frost layer through condensate distribution, PhD Dissertation, University of Illinois at Urbana-Champaign, USA, 2001.
[16] Z.L. Liu, X.H. Zhang, H.Y. Wang, S. Meng, S.Y. Cheng, Influences of surface hydrophilicity on frost formation on a vertical cold plate under natural convection conditions, Exp. Therm. Fluid Sci. 31 (7) (2007) 789–794.
[17] X.M. Wu, W.C. Wang, Theoretical analysis of initial behavior of frost formed on a cold surface, J. Eng. Thermophys. 24 (2) (2003) 286–288.